

Enhancement Performance of DSTATCOM depending on PV System Supply control

Abstract. This article examines the impacts of a transient analysis of a compensator of static synchronous on a system of distribution power (DSTATCOM) on power quality when a PV system DC input source is utilised to supply the system. Due to the nature of these sources' operation, including renewable energy on the input power supply has a variety of ramifications for DSTATCOM's operation. In order to understand the variance in temporal response and its impact on the compensatory process, the dynamic response of the distribution system is investigated under the influence of both battery and PV system sources (PV-Battery). Renewable energy is connected across the dc-link capacitor channel to characterize their impact on the power system's dynamic performance. In this study, three scenarios were investigated: first, photovoltaic (PV) cells are connected solely via the dc-link, second, battery storage is connected solely, and third, a PV system structure (PV cells + battery storage) is explored. DSTATCOM is used to compensate for the reduction in reactive and active power that happens during balanced and unbalanced operation of non-linear loads. The presence of a renewable source enhances the system's power quality by reducing the current source's harmonic components. The Star / Delta transformer is also used to split the three-phase legs of the DSTATCOM VSC, providing a channel for the fundamental zero sequence and a balanced three-phase current. STATCOM control circuit based on synchronous reference frames (SRF).

Streszczenie. W niniejszym artykule zbadano wpływ analizy stanu nieustalonego kompensatora synchronicznej statycznej na system zasilania dystrybucyjnego (DSTATCOM) na jakość energii, gdy źródło wejściowe DC systemu fotowoltaicznego jest wykorzystywane do zasilania systemu. Ze względu na charakter pracy tych źródeł, uwzględnianie energii odnawialnej na zasilaniu wejściowym ma różne konsekwencje dla pracy DSTATCOM. Aby zrozumieć wariację odpowiedzi czasowej i jej wpływ na proces kompensacyjny, badana jest dynamiczna odpowiedź systemu dystrybucyjnego pod wpływem zarówno źródeł baterii, jak i systemu PV (PV-Battery). Energia odnawialna jest podłączona przez kanał kondensatora dc-link, aby scharakteryzować ich wpływ na dynamikę systemu zasilania. W niniejszym badaniu zbadano trzy scenariusze: po pierwsze, ogniwa fotowoltaiczne (PV) są połączone wyłącznie za pośrednictwem łącza prądu stałego, po drugie magazynowanie baterii jest podłączone wyłącznie, a po trzecie, zbadano strukturę systemu PV (ogniwa fotowoltaiczne + magazynowanie baterii). DSTATCOM służy do kompensacji redukcji mocy bierniej i czynnej, która ma miejsce podczas pracy zrównoważonej i niezrównoważonej obciążen nieliniowych. Obecność źródła odnawialnego poprawia jakość zasilania systemu poprzez redukcję składowych harmonicznych źródła prądu. Transformator gwiazda/trójkąt jest również używany do rozdzielania trójfazowych odgałęzień DSTATCOM VSC, zapewniając kanał dla podstawowej sekwencji zerowej i zrównoważonego prądu trójfazowego. Obwód sterowania STATCOM oparty na synchronicznych ramach odniesienia (SRF). **(Poprawa wydajności DSTATCOM w zależności od sterowania zasilaniem systemu fotowoltaicznego)**

Keywords DSTATCOM, PV, MPPT, SRF and VSC

Słowa kluczowe: system fotowoltaiczny, DSTATCOM, VSC

Introduction

Renewable sources of energy (RSE) have emerged as the preferred answer to power system challenges. As a result, current efforts place a premium on improving the performance of various energy source kinds. The process of getting, utilising, and consuming this energy correctly results in high power quality systems. It is critical to minimise losses in order to get a timely reaction of power compensation from a renewable energy source. [1, 2]. The photovoltaic generated electricity acquired from solar cell sources is variable and influenced by weather circumstances such as variations in solar radiation as well as the effect of high temperatures, etc[3]. A MPPT algorithm is introduced to obtain a maximum power generated by solar panels [4]. Maximum power can be created using a variety of methods that also improve overall system efficiency. The Observe and Perturb (O &P) approach, method of perturb and observe, the open-circuit voltage method, and the constant voltage method are among the present work's strategies [5, 6]. The P&O approach is connected to a DC-DC boost converter circuit to generate the switch ON/OFF pulse of an Insulated Gate Bipolar Transistor (IGBT). To obtain generated extreme power, the circuit of boost is connected across the PV cells[7]. The solar cells' generated power is delivered into the STATCOM input Dc voltage link via the boost Dc-Dc circuit. Extra power generated by PV cells is stored in an energy storage unit (battery) [8]. The battery-stored energy is used to power the compensator's input DC voltage connection during night intervals or in severe weather conditions where

solar radiation is very low or absent. A buck-boost circuit is used to regulate the battery output voltage and enhance the charge/discharge cycle to achieve high charge and discharge accuracy. To provide consistent coordination performance between PV and battery operation, a logic circuit is used [9-13].

To regulate the compensation of DSTATCOM, the synchronous reference frame theory with unit vector approach is considered [14, 15]. Three-phase four-wire distribution systems have a number of power quality concerns due to harmonics caused by non-linear loads, unbalance in the neutral load, and other reasons [14]. IGBT devices utilised as switching transistors in the VSC provide a quick reaction for the inverter output voltage, which improves DSTATCOM correction performance. [16]. A number of compensating devices are used to improve power quality, voltage profile, power factor, and total harmonics (THD) distortion factor. The Static Var Compensator (SVC) is one of them, and it is regarded as a classic kind because it relies on a big capacitor and inductance for correction [17]. The introduction of more advanced SVC gear has stemmed from the quick advancement of power electrical gadgets. It is distinguished by its tiny size, quick compensating response, and controllability. These devices include the static synchronous compensator (STATCOM), static synchronous series compensator (SSSC), and unified power flow controller (UPFC). The UPFC is the finest compensator among all flexible a.c transmission system (FACTS) devices. The composite control circuits and high production costs are

disadvantages [18-19]. In the current work, a STATCOM device was used to improve power quality because its control circuit is simpler than that of a UPFC, it is small in size, and it has a high compensating capability [20]. The unit vector approach of the SRF is well suited for manipulating the DSTATCOM control circuit [22, 23].

The study's contribution is summed up in a high coordination of PV system supply system. They collaborate as a PV system system to supply DSTATCOM's needed DC link voltage.

This study examines and assesses the effects of DSTATCOM time response of power compensation when different types of supply sources are linked across the DC link input voltage. Four approaches are considered. First, the DSTATCOM with DC input voltage alone is utilised; second, the PV panel is supplied with the DC voltage channel; third, the battery storage unit is regarded to supply the DC voltage link; and finally, the STATCOM DC input voltage is supplied by a PV system PV-battery storage unit. An analysis of the proposed compensatory power sources reveals that the DSTATCOM input voltage is determined by which sources attain steady state first.

Methodology of PV system with DSTATCOM

A multi-sources compensation system (PV-battery storage unit) is an effective method for improving dynamic response and compensating for power quality reductions (low power factor, high THD, injected harmonics current components, low stability, low response time, and so on) caused by non-linear loads and system distribution disturbances. During the compensation stage, a good coordination design is required. The PV system sources' performance is analyzed and evaluated to indicate their impact on the distribution system. As a compensation device, a DSTATCOM voltage source inverter (VSI) with IGBT solid-state switches is used. In this paper, the compensator's control methodology is based on synchronous reference frame with unit vector technique.

Constriction of DSTATCOM with PV system

Fig1 depicts the DSTATCON distribution power system design with control method (SRF and unit vector) based on PV system input DC voltage sources. The photovoltaic boost converter and battery back-boost converter power the multi-source power supply. The grid is linked to the DSTATCOM compensating system with star/delta transformer at a common coupling point [22].The non-linear load that is consist of three-phase inverter is connected to the system. This system supplied by DC voltage source V_{dc} connected across the capacitor where its value can be calculated using Equ. 1.

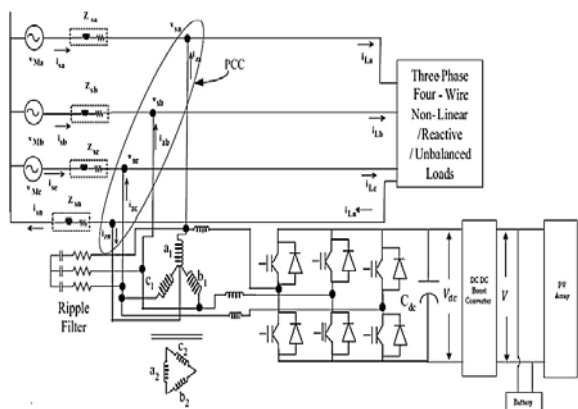


Fig 1. Schematic Diagram of DSTATCOM is fed by a PV system with two sources (PV and battery).

The DC value of input voltage V_{dcact} across the capacitor, which is employed to supply the VSC inverter, is obtained using the instant power fed to the DSTATCOM is calculated using Equ. One [22]:

$$(1) \quad V_{dcact} = \frac{2\sqrt{2}V_{LL}}{\sqrt{3} * m}$$

In addition, the DC-link capacitance C_{dc} that is connected across the input of DSTATCOM is formulated as shown in Equ. Two [23]:

$$(2) \quad 0.5 C_{dc} \left[(V_{dc_{ref}}^2) - (V_{dc_{actual}}^2) \right] = 3V_{ph}(OLI_{ph})t$$

The phase voltage of the considered power system is computed based on Equ. 3 as follows:

$$(3) \quad V_{ph} = \frac{V_{Line}}{\sqrt{3}}$$

where: m is the modulation index that is normally suppose equal to 1, $V_{dc_{ref}}$ is the DC reference input voltage which is assuming about 680 V, $V_{dc_{act}}$ is the actual input voltage of STATCOM DC which is equal to 678.69 V. V_{LL} is the line-line power system voltage where it is assumed equal to 415 V, C_{dc} is the DC connection input channel capacitor and equal 2900 μF , OL over load factor where it is assumed equal to 1.2, I_{ph} is the grid phase current and it is assumed equal 57.14 A, V_{ph} is the phase voltage and it is equal 240 V, the recovery time of DC connection voltage equal 355 μs .

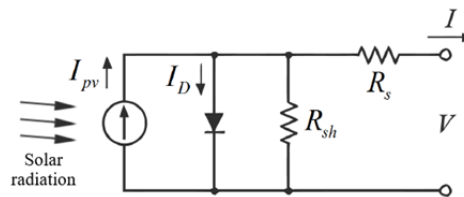


Fig 2. PV system equivalent circuit

Modeling of PV panel

Fig 2 [21] depicts the comparable circuit of a PV renewable energy system. A dc-dc boost converter connects the PV module to the common input voltage dc bus. Sanyo solar modules make up the PV system. These solar modules are wired in series to form groups, then in parallel to form the PV array. The solar module in Fig2 is a current source with a parallel diode. PV farms use maximum power point tracking (MPPT) technology to ensure maximum solar energy generation. The DC-DC boost converter's triggering gate is used as a controller to attain the highest output PV array voltage. Different MPPT procedures for solar PVs have been investigated; the current study uses a Perturb & Observe (P&O) methodology. The output PV voltage is always regulated to attain a maximum voltage for varying solar irradiation variations due to the influence of MPPT. As a result, the generated PV is at its peak under sun radiation. Table 1 [24] lists the V-I specs.

Table 1. The datum of solar panel model at 1000 W/m² and temperature of 25°C.

Parameters	TYPE
Power max	240 W
Open circuit voltage	37 V
Current of short circuit	8.3 A
Maximum power voltage (V.pm)	30 V
Maximum power current (I.pm)	6.65 A
Temperature coefficient. of short circuit current	46 mA/°C
Open circuit voltage coefficient of Temperature.	- 0.109V/°C

The following relationships summarise the fluctuation in solar irradiation [21].

$$(4) \quad I = I_{pv} - I_o \left[\exp \left(\frac{V_{oc} q}{N_c K t} \right) - 1 \right] - \frac{V_{oc}}{R_{SH}}$$

$$(5) \quad V_{oc} = V + R_S I$$

The PV modul current is calculated using the following equation, which is dependent on two factors: the linear variation of solar irradiation and the temperature.

$$(6) \quad I_{pv} = (I_{pv,s} + K_t \Delta_t) \frac{g}{g_s}$$

The $I_{pv,s}$ value is evaluated using equation (7) as shown in Fig. 2:

$$(7) \quad I_{pv,s} = \frac{R_{SH} + R_S}{R_{SH}} I_{SH}$$

Where: (I_{pv}) and (I_o) are the PV current and initial current of one cell respectively, where the number of cells that connected (N_c), (K) is the boltzmann constant and it is to (1.38065×10^{-23} J/K), (t) is temperature of one cell, (q) is the PV electronic and equal (1.60217×10^{-19} eC), (R_{SH}) is the electrical circuit's shunt resistance, (R_S) is the electrical circuit's series resistance, (i) is the PV cell factor where its range equal 1 in current work, ($I_{pv,s}$) is the photo condition current, (K_t) per temperature, is the coefficient current, (Δ_t) is the actual and normal temperatures difference b, and (g, g_s) are the panel surface irradiation and normal irradiation, respectively [19].

DC link voltage control Approaches

There are two types of circuits for control of a DC link's voltage are as follows:

Boost converter circuit of Photovoltaic

The output power of PV cells had to be adjusted constantly when considering the DC-DC boost converter circuit. Fig3 illustrates this [25], this circuit is convenient for controlling the input DC Link supply voltage for VSI in response to variations in the applied load.

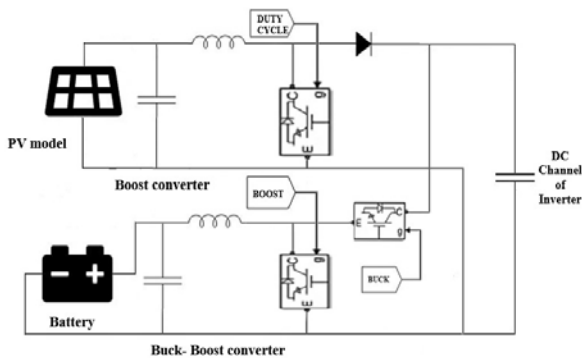


Fig 3. Schematic diagram coordination between PV boost circuit and battery buck-boost circuit.

Maximum power point tracking (MPPT) Technique

As previously indicated, the Perturb & Observe Technique (P&O) is being used in current research to achieve MPPT of output-generated power [23]. P&O is used to achieve the control IGBT train pulses interval (D) [24].

$$(8) \quad \frac{dI_{pv}}{dV_{pv}} = - \frac{I_{pv}}{V_{pv}}$$

$$(9) \quad \frac{dI_{pv}}{dV_{pv}} \geq \frac{I_{pv}}{V_{pv}}$$

$$(10) \quad \frac{dI_{pv}}{dV_{pv}} \leq \frac{I_{pv}}{V_{pv}}$$

Where: (V_{pv}, I_{pv}) represent the voltage and current of the PV respectively, (dV_{pv}, dI_{pv}) are the average change values of PV voltage and current respectively. When the derivative in equation (8) equals zero, the MPP scenario is obtained. If the power is less than MPP, the calculation says When the derivative in equation (8) equals zero, the MPP scenario is obtained. If the power is less than MPP, the V_{pv} value must be increased to attain MPP, according to the equation (9). If the PV produced power is more than the MPP, the V_{pv} must be reduced to reach the MPP situation, according to equation (10).

DC to DC buck-boost

Since of its deep charging duration and substantial available capacity, lead acid batteries are used in conjunction with PV arrays because they are more common and compatible with many types of inverters [25, 26]. When the generated power from the solar panels exceeds the demand load, the buck circuit converter absorbs the excess solar electricity. In the absence of a solar panel or when generation is small, the boost circuit kicks in to compensate for the power shortfall, as shown in Fig(2).

The following equations [11] can be used to explain the charge/discharge charging lead acid battery cycle:

$$(11) \quad V_{B_{dis}} = V - Ri_b - k \frac{Q}{Q-i(t)} (i(t) + t^f) + \exp(t)$$

$$(12) \quad V_{B_{ch}} = V - Ri_b - \left[k \frac{Q}{i(t)-0.1Q} \right] i^f - \left[k \frac{Q}{Q-i(t)} \right] i(t) + x p(t)$$

$$(13) \quad i(t) = \int i_b d(t)$$

Where: ($V_{B_{ch}}, V_{B_{dis}}, V$) are represent charge/discharge voltage of the battery and battery constant voltage respectively (V), (k) is the constant of polarisation (V/Ah), (Q) is the capacity of battery (Ah), ($i(t)$) is the actual current of battery charging (A/h) and calculate according to equation (16). (i_b) is the battery current (A), (i^f) is the current of filter (A) and (t^f) is the time of filter (h).

Control algorithm of DSTATCOM

To Various control structure methods are utilised to replicate the DSTATCOM reference source currents (i_{sref} , i_{sbref} , and i_{scref}) control circuits. synchronous reference frame (SRF) theorems, decoupled current control, and instantaneous reactive power theorems (p-q theory). A SRF was used in the current work [14, 15, 29, 30, 31] in the present paper.

The voltages of DSTATECOM's three phases are monitored at the common coupling point. $V_{abc-PCC}$

As illustrated in equations (18) and (19), the error signal is routed to a second PI controller, whose outputs are transformed to reference currents in the q-axis I_q . The Clark and Park transformation matrices are necessary to convert the three-phase system to a d-q system and then evaluate the control signal's reference currents value. The three phase load currents are used as a reference signal to determine the actual current values in the d-q axis (i_d^* , i_q^*) using sensors. In the equation, the transformation matrix is described (20). A DC Link voltage signal sensor which fixed on the capacitor link of VSC is used to provide the voltage signal of DC V_{dc} . The error signal evaluated from subtracting the V_{dc} from the DC reference voltage ($V_{dc_{ref}}$) is transformed to current signal (losses of switches VSC) using first PI controller as defined in the equations (21) and (22). In the last stage, the real current (i_q) adds to (i_{qdc}) which form the reference current (i_q^*) while the actual current (i_{adc}) adds to losses current (i_{loss}) which produce the reference current (i_d^*) as explain in Fig. 6 [32]. Then an inverse transformation is applied on reference

currents i_{d_ref} and i_{q_ref} to compute the three phase reference currents ($i_{abc.ref}$). The resulted three phase currents are compared with source currents that contains an injected load currents harmonics where the generated signals is used to produce appropriate switching signals for turn ON/OFF the gates of IGBTs switches.

$$(18) \quad i_{q(n)} = i_{q(n-1)} + K_{pq}(V_{AE(n)} - V_{AE(n-1)}) + K_{iq} v_{AE(n)}$$

$$(19) \quad i_{q^*} = i_{qdc} + i_{qr}$$

$$(20) \quad \begin{bmatrix} i_{d^*} \\ i_{q^*} \\ i_o \end{bmatrix} = \begin{bmatrix} \sin \theta & \sin(\theta - \frac{2\pi}{3}) & \sin(\theta + \frac{2\pi}{3}) \\ \cos \theta & \cos(\theta - \frac{2\pi}{3}) & \cos(\theta + \frac{2\pi}{3}) \\ \frac{1}{6} & \frac{1}{6} & \frac{1}{6} \end{bmatrix} \begin{bmatrix} \frac{2+iLa}{3} \\ \frac{2+iLb}{3} \\ \frac{2+iLc}{3} \end{bmatrix}$$

$$(21) \quad i_{d^*} = i_{d dc} + i_{loss}$$

Where: ($V_{AE(n)}$) is the error signal generated by compare the reference (V_s^*) with sensed grid voltage signal. ($V_{dcE(n)}$) is the signal of error resulted from subtracting the reference and sensed signals of DC link voltage for nth sample. (K_{idd}, K_{pdd}) are represent gain factors of intgral and proportional of first PI controller of DC link voltage. (K_{iqt}, K_{pqt}) are the gain factors of intgral and proportional of the s

second PI controller at PCC.

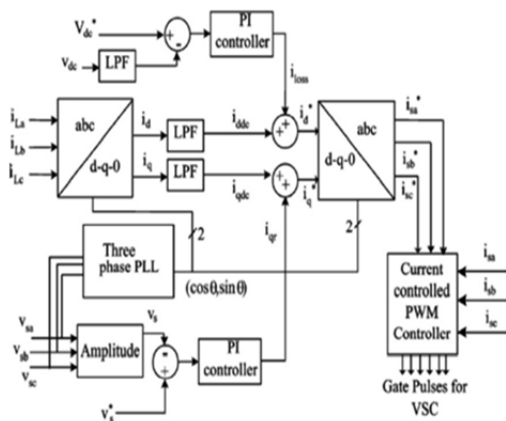


Fig.6. Schematic diagram of DSTATCOM control circuit using SRF.

Results and Discussion

A PV system configuration is connected across the DC link input voltage of DSTATCOM using MATLAB SIMULINK 2018a to simulate the DSTATECOM compensator with control circuits. A three-phase four-wire grid with a synchronous generator of kVA provides power to the non-linear demand in the considered power system. Table 2 lists the values of all components used in the current design.

Table.2 Parameters of the design work

Parameters system	DATUM
Frequency and Three-phase voltage of Grid	50Hz ,415V
Impedance of Line Per Phase (R_s, L_s)	0.01 Ω , 2 mH
Non-linear Load (Three phase bridge rectifiers with RL)	130 Ω , 10mH,
Ripple filter (R_f, C_f).	5 Ω , 5 μf
Ac inductor	3.3 mH
DSTATCOM capacitor of Dc-link	2900 μf
DSTATCOM voltage of Dc-link	680 V
Dc PI.1 (K_{pdd}, K_{idd})	0.2, 1
PCC voltage PI.2 (K_{pq}, K_{iq})	0.01, 2
PI controller of logical coordination circuit (KP, KI)	0.8×10^{-9} , 0.8×10^{-8}
Current and Voltage of Battery (V_b, I_b)	550V, 13Ah

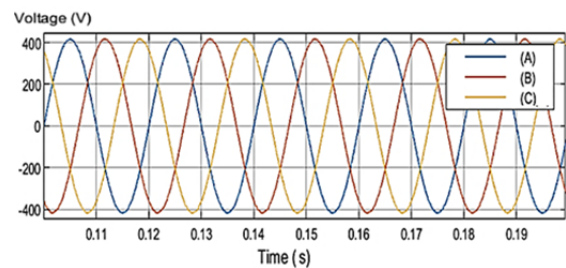


Fig 7. Three-phase synchronous generator supply a non-linear load without DSTATCOM compensation Voltage waveform.

In Fig 8 the three phase current waveform without compensation is present.

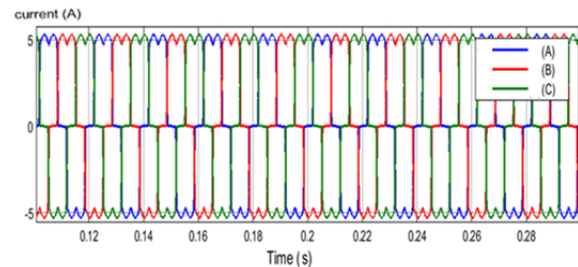


Fig 8. Three-phase current source before compensation.

Fig 9 shows the THD% for three phase current of source before the compensation.

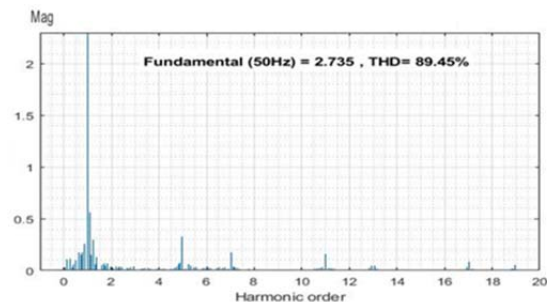


Fig 9. The THD% of three phase current source before compensation.

When the STATCOM is powered by a battery, Fig. 10 displays the time response of the compensation effect for dc-link voltage. The settling time is 0.07s, and the influence of cut-off wires on the VSC dc-link voltage for DSTATCOM is absent.

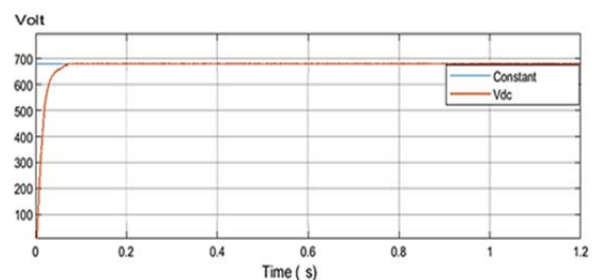


Fig 10. DC link channel voltage time response when

The DSTATCOM is fed from the PV system energy sources. Table 3 shows the response times for all potential energy sources for DSTATCOM's dc-channel. The PV system system, when compared to the other sources, clearly provides a greater response. When employing Arduino sensors and the value of current source 31A, Fig11 displays the three phase current of the source after compensation.

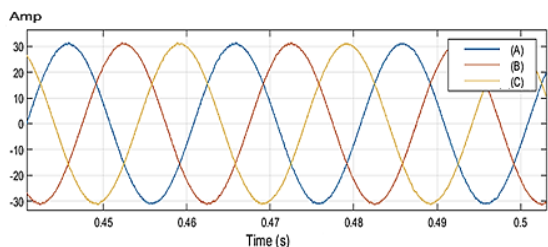


Fig 11. Three phase currents of source after compensation of DSTATCOM with PV system.

Fig12 shows that the supply source's active power is 16.1 KW, while DSTATCOM's active power is 26.75

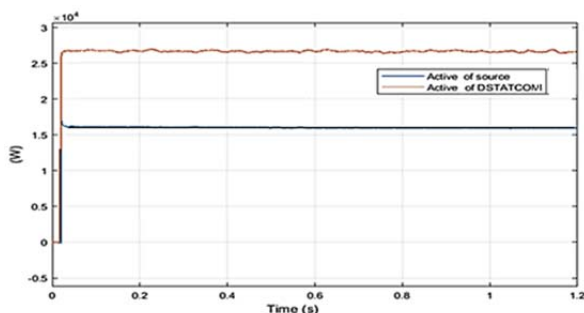


Fig 12: The active power of supply source and DSTATCOM using Arduino sensors.

Fig13 shows the THD% proportion for three phase current supply source with compensation.

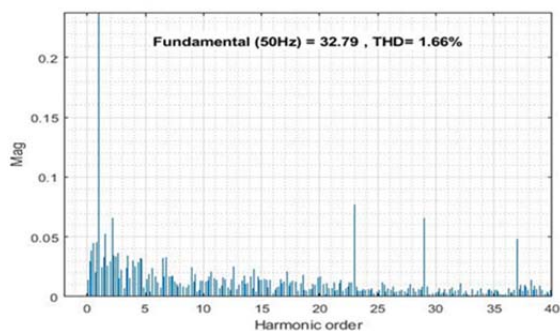


Fig 13. THD% proportion for three-phase current of supply source with compensation.

Conclusion

Different types of DC power sources were studied in order to assess the capabilities of the static synchronous compensator used in the distribution grid to improve its dynamic performance during active and reactive power shortages. The proposed technique is motivated primarily by the need to improve power quality. Because of disruptions caused by faults, unbalanced loads, adding or removing loads from the grid, the nonlinearity of three-phase loads (many types of converters), or transient operation in such phases following the operation of large induction machines A quick reaction system implies that The generator unit as well as the loads will run smoothly. The temporal reaction of active/reactive power systems under different types of PV systems DC sources offer three-leg VSC for (DSTATCOM) has been studied and compared. The STATCOM DC link voltage was supplied via the PV system PV-battery system using a high coordination logical circuit. The performance of the PV system's energy sources was compared to that of a constant dc-link voltage. The findings indicate that the PV system energy sources system responds more quickly. In addition, the DSTATCOM compensation issue for source currents and THD for phase

are improved when compared to the performance of a constant DC voltage supply.

Authors

Ayman Dhafer Abdul-Nafa

I have graduated from Medical Instrumentation Technology Engineering Department Of Technical Engineering College Of Mosul at Northern Technical University. I get a master degree of technology in Medical instrumentation Technique Engineering of Electrical Engineering Technical College at Middle Technical University. I am working as assistant lecture in college of dentistry in university of Mosul 2021. ayman@uomosul.edu.iq

Suha Sabeeh Ahmed

I have graduated from Medical instrumentation Technique Engineering of Electrical Engineering Technical College at Middle Technical University at 2006. I get a master degree of technology in Medical instrumentation Technique Engineering of Electrical Engineering Technical College at Middle Technical University. I am working as assistant lecture in Electrical Engineering Technical College at Middle Technical University 2021. suhasabeh@mtu.edu.iq

REFERENCES

1. S. A. Khajehoddin, et al., "DC-Bus Design and Control for a Single-Phase Grid-Connected Renewable Converter with a Small Energy Storage Component," IEEE Transactions on Power Electronics, Vol. 28, No. 7, pp. 3245-3254(2013)
2. S. Taghizadeh, et al., "A Fast and Robust DC-Bus Voltage Control Method for Single-Phase Voltage-Source DC/AC Converters," IEEE Transactions on Power Electronics, Vol. 34 (9), pp. 9202 – 9212, 26 November 2018.
3. F. Abed and Yarub Al-Douri, "Review on the energy and renewable energy status" Renewable and Sustainable Energy, vol. 39, pp. 816-827.
4. P. Bhatnagar and R.K. Nema, "Maximum power point tracking control techniques: State-of-the-art in photovoltaic applications," Renewable and Sustainable Energy Reviews, Vol. 23, pp.224–241, July 2013.
5. D. F. Liu, et al., "A Variable Step Size INC MPPT Method for PV Systems," IEEE TRANSACTIONS ON INDUSTRIAL ELECTRONICS, VOL. 55, NO. 7, JULY 2008, pp.2622-2627.
6. D. Verma, et al., "Maximum power point tracking (MPPT) techniques: Recapitulation in solar photovoltaic systems," Renewable and Sustainable Energy Reviews, Vol.54, pp.1018–1034, February 2016.
7. S. K. Changchien, et al., "Novel High Step-Up DC–DC Converter for Fuel Cell Energy Conversion System," IEEE Transactions on Industrial Electronics, Vol.57 No.6, pp.2007–2017, JUNE 2010.
8. O. P. Mahela, et al., "Power quality improvement in distribution network using DSTATCOM with battery energy storage system," Electrical Power and Energy Systems, Vol. 83, pp. 229–240, December 2016.
9. I. Ranaweera, et al., "Residential photovoltaic and battery energy system with grid support functionalities," International Symposium on Power Electronics for Distributed Generation Systems (PEDG), 2015 IEEE 6th.
10. N. Prakash, et al., "Power quality improvement of grid inter connected PV system system using STATCOM," International Journal of Advanced Engineering Technology, Vol.7 No.2, pp.1225-1233, April-June 2016.
11. S and L. F, "Coordinated V-f and P-Q Control of Solar Photovoltaic Generators with MPPT and Battery Storage in Microgrids," IEEE Transactions on Smart Grid, Vol. 5 No. 3, PP. 1270–1281, May 2014.
12. M. Aryanezhad, Elahe Ostadaghaee and Mahmood Joorabian, "A novel simplified approach to complexity of power system components including nonlinear controllers based model reduction", International Journal of Electrical Power & Energy Systems, Vol. 73, December 2015, Pages 298-308.
13. E. Dursun and O. Kilic, "Comparative evaluation of different power management strategies of a stand-alone PV/Wind/PEMFC PV system power system," International Journal of Electrical Power & Energy Systems, Vol. 34, pp. 81–89, 2012.
14. N. Geddada, et al., "Synchronous reference frame based current controller with SPWM switching strategy for

- DSTATCOM applications," IEEE International Conference on Power Electronics, Drives and Energy Systems, pp.16-19, December 2012
15. A. K Pandey, et al., " Compensation of neutral current using unit vector template method-based control algorithm for DSTATCOM to power quality improvement," International Journal of Science Engineering and Technology, Vol.6 NO. 2, pp. 154-159, 2018.
 16. J. M. MAZA-ORTEGA, et al., " Overview of power electronics technology and applications in power generation transmission and distribution," Journal of Modern Power System and Clean Energy, Vol.5 No. 4, pp. 499–514, 13 July 2017.
 17. Aryanezhad M, "Management and coordination of LTC, SVR, shunt capacitor and energy storage with high PV penetration in power distribution system for voltage regulation and power loss minimization", International Journal of Electrical Power & Energy Systems, Vol 100, September 2018, Pages 178-192.
 18. M. S. El-Moursi, et al., "Novel Controllers for the 48-Pulse VSC STATCOM and SSSC for Voltage Regulation and Reactive Power Compensation," *IEEE Transactions on Power Systems*, vol. 20, no. 4, pp. 1985–1997, Nov. 2005.
 19. M. Aryanezhad, Elahe Ostadaghaee and Mahmood Joorabian, "Management and coordination charging of smart park and V2G strategy based on Monte Carlo algorithm", Smart grid conference (SGC); IEEE published, 2014. p. 1-8.
 20. M. N. Kabi, et al., "Coordinated control of grid connected photovoltaic reactive power and battery energy storage systems to improve the voltage profile of a residential distribution feeder," *IEEE Transactions on Industrial Informatics*, Vol.10 No.2, pp. 967–977, July 2014.
 21. B.N. Singh, et al., "Design, simulation and implementation of three-pole / four-pole topologies for active filters," *IEE Proceedings - Electric Power Applications*, VOL.151 (4), July 2004, pp.467–476.
 22. B. Singh and S. R. Arya, " Design and control of a DSTATCOM for power quality improvement using cross correlation function approach," *International Journal of Engineering, Science and Technology*, Vol. 4, No. 1, 2012, pp. 74-86.
 23. <<SANYO_HIT240_235_HDE4_Datasheet.pdf >> .
 24. S.Gomathy, et al., "Design and implementation of Maximum Power Point Tracking (MPPT) algorithm for a standalone PV system," *International Journal of Scientific & Engineering Research* Vol. 3, No.pp. 1-7, March -2012
 25. S. Y. Prasad, et al., " Microcontroller based intelligent DC/DC converter to track Maximum Power Point for solar photovoltaic module," *IEEE Conference on Innovative Technologies for an Efficient and Reliable Electricity Supply*, pp.94-101, 4 November 2010.
 26. N. Omar, et al., "Lithium iron phosphate based battery Assessment of the aging parameters and development of cycle life model," *Applied Energy*, pp.1575–1585, 13 January 2014.
 27. P. Horkos, et al., "Review on Different Charging Techniques of Lead- Acid Batteries," *Third International Conference on Technological Advances in Electrical, Electronics and Computer Engineering (TAECE)*, April 2015, pp.27-32, April 2015.
 28. T.sukanth, et al., " Comparative Study Of Different Control Strategies For DSTATCOM ," *International Journal of Advanced Research in Electrical, Electronics and Instrumentation Engineering*, Vol. 1(5), November 2012, pp.362-368.
 29. R. S. Herrera and P. Salmerón, " Instantaneous Reactive Power Theory: A Reference in the Nonlinear Loads Compensation," *IEEE Transactions on Industrial Electronics*, Vol. (56)6, June 2009, PP.2015-2022.
 30. M. K. Ghartemani, et al., " Problems of Startup and Phase Jumps in PLL Systems," *IEEE Transactions on Power Electronics*, 27(4), APRIL 2012, PP. 1830–183.
 31. V. K. Kannan, et al., " Photovoltaic based distribution static compensator for power quality improvement," *Electrical Power and Energy Systems*, Vol.42, 16, pp. 685–692, 16 June 2012.
 32. D. B Kanase, et al., "Distribution Static compensator for Power Quality Improvement using PV Array", *IEEE International Conference on Electrical, Computer and Communication Technologies (ICECCT)*, 27 August 2015.